

# An improved hybrid AC to DC converter suitable for electric vehicles applications

Khaled A. Mahafzah<sup>1</sup>, Mohamad A. Obeidat<sup>2</sup>, Hesham Alsalem<sup>3</sup>, Ayman Mansour<sup>4</sup>,  
Eleonora Riva Sanseverino<sup>5</sup>

<sup>1</sup>Department of Electrical Engineering, Faculty of Engineering, Al-Ahliyya Amman University, Amman, Jordan

<sup>2</sup>Department of Electrical and Mechatronics Engineering, Faculty of Engineering, Tafila Technical University, Tafila, Jordan

<sup>3</sup>Department of Mechanical Engineering, Faculty of Engineering, Tafila Technical University, Tafila, Jordan

<sup>4</sup>Department of Computer and Communications Engineering, Faculty of Engineering, Tafila Technical University, Tafila, Jordan

<sup>5</sup>Department of Engineering, University of Palermo, Palermo, Italy

## Article Info

### Article history:

Received Oct 24, 2024

Revised Apr 17, 2025

Accepted Jul 3, 2025

### Keywords:

EV charging

Flyback

HVDC grid

Hybrid converter

SEPIC

## ABSTRACT

This paper introduces a novel hybrid AC-DC converter designed for various applications like DC micro-grids, electric vehicle (EV) setups, and the integration of renewable energy resources into electric grids. The suggested hybrid converter involves a diode bridge rectifier, two interconnected single ended primary inductor converter (SEPIC) and Flyback converters, and two additional auxiliary controlled switches. These extra switches facilitate switching between SEPIC, Flyback, or a combination of both. The paper extensively discusses the operational modes using mathematical equations, deriving specific duty cycles for each switch based on the circuit parameters. This hybrid converter aims to decrease total harmonic distortion (THD) in the line current. The findings exhibit a THD of approximately 14.51%, showcasing a 3% reduction compared to prior hybrid converters, thereby enhancing the power factor of the line current. Furthermore, at rated load conditions, the proposed converter achieves 90% efficiency. To validate the proposed hybrid converter's functionality, a 4.5 kW converter is simulated and performed using MATLAB/Simulink after configuring the appropriate passive parameters.

*This is an open access article under the [CC BY-SA](https://creativecommons.org/licenses/by-sa/4.0/) license.*



## Corresponding Author:

Khaled A. Mahafzah

Department of Electrical Engineering, Faculty of Engineering, Al-Ahliyya Amman University

Amman 19328, Jordan

Email: k.mahafzah@ammanu.edu.jo

## 1. INTRODUCTION

Global warming, fuel emissions, fuel prices, and politics have moved customers' attention to more dependable and environmentally beneficial renewable and friendly energy sources. With over 95 million cars sold each year, the transportation sector contributes more than 24% of global emissions [1]. California, England, France, Germany, and many European countries will ban selling conventional internal combustion engine vehicles starting from 2035 and after.

Recent technology improvements in power electronics and the utilization of these advancement in transportation plays a major role for the wide spread of electric vehicles (EV) later on [1], [2]. Demands of EVs increased rapidly and manufacturers started to enhance their efficiencies and competencies. Depending on the source of electricity used to charge EV, emissions from EV can decreased to up to 90% compared to emissions from ICE. EV mainly consist of different components such as the rechargeable battery, power inverters,

electric traction motor, power electronics controller, charging port, and transmission. The rechargeable battery (voltages vary from 200 V to 450 V) that passes DC voltage to the inverter. Power inverters changes the current from DC current to an AC current [3]. Electric traction motor turns the transmission and the traction wheels, and the power electronics controller works as a converter/inverter combination.

The charging port allows the EV to be connecting to an external source to charge the traction battery pack whenever needed. There are four major types of EVs; battery electric vehicle or all electric vehicle (BEV or EV), hybrid electric vehicle (HEV), plug in hybrid electric vehicle (PHEV), fuel cell electric vehicle (FCEV) [1]-[3]. EV is a noise free vehicle, with the most efficient components that overcome all ICEs [4]-[6].

EVs can be divided into three main subsystems categories [1], [7], [8]. First, the high voltage circuit which includes the rechargeable battery between 200 to 800 volts, contractors which relay power to motor which propel the vehicle controlled by inverters, DC to DC converter, on board charging unit, smart shunt used for battery managements and can bus which control power delivery and implement performance and safety features. Second, low-voltage circuit, which is responsible for operating the accessory device through rear PDU-8 which programmed to activate the inverters cooling pump, taillight blinkers and reverse light. Front PDU-8 controls the CAN keypad, digital dash display accurately. Two additional PDU-8 used to activate the contractors for the high voltage systems and control the headlights. Third, multiple can networks. Which allows multiple devices to share data between the networks and guarantee an optimal and safe performance.

Inverters can be the key solution in the field of hybrids and electrical vehicles. The motor in hybrid and EVs utilize three phase voltage source inverters (VSI) based on insulated gate bipolar transistors IGBTs made of silicon carbides or gallium nitrides to turn on and off within few micro or nano-seconds [9], [10]. The exploration of a three-phase modular differential inverter (MDI) integrating single ended primary inductor converter (SEPIC) modules and SiC devices is discussed, delivering AC power to the grid with enhanced efficiency and reduced total harmonic distortion (THD) through high-frequency switching and modular flexibility [11]. Takaoka *et al.* [12] introduces of an isolated DC to single-phase AC converter that incorporates active power decoupling using a coupled inductor and interleaved boost converter, achieving independent control of power conversion, an 84.5% reduction in second-order harmonics, and a maximum efficiency of 94.5%. Larouci *et al.* [13] examines a flyback converter using a mixed conduction mode, balancing efficiency and transformer volume by combining discontinuous and continuous conduction modes within an optimized control framework, favoring continuous conduction for efficiency and discontinuous conduction to minimize component volume. Collectively, these studies advance power conversion technologies by enhancing grid-connected system efficiency, reducing harmonic distortions, and optimizing design approaches for improved performance and scalability.

Another type of inverters is the current source inverters (CSI) with the aid of a capacitor filters to regulate the distortion currents. Z source inverter (ZSI) is an inverter that combine both VSI and CSI. The produced voltage from ZSI is either higher or lower than the input voltage source. Three level inverters used in EV with switches that are more efficient especially for moderate to high frequency levels with lower voltage distortion and higher motor efficiency. Insulated gate bipolar transistors (IGBTs) is a major part used in inverters [14]-[18]. Power module as well as gate drivers are responsible for the dynamic behavior of the diodes. Current sensor and DC link capacitor are components used in inverters as a means of protection and better performance control [19]. All inverters are equipped with a thermal management system to control Temperature through cooling system (water-cooling or forced air-cooling). Chevrolet MY2016 Volt used traction power inverter module (TPIM) with dual VSIs and wide bandgap (WBG) [20]. Toyota MY2016 Prius used two VSIs, a boost converter. Nissan MY2012 LEAF used a single VSI. Tesla model S uses 5.8kg 6.4L, TO-247 water-cooled inverter. Different generations of inverter were used by each individual EV Automaker to overcome shortcomings from previous models and have an improved performance. Some EV and HEV has different types of inverters that perform as an inverter/converter assembly that works as boost converter, boost converter module, and the coil that produce the voltage higher than battery voltage. EVs and PHEVs tend to have higher power inverters in the range of 100–500 kW compared to the 30 to 60 kW range in HEV [5], [21], [22].

In response to the demand for advanced power electronics systems tailored specifically for EVs, this paper introduces a cutting-edge hybrid AC-DC converter, redefining the landscape of energy conversion technology. Recognizing the need for a more nuanced focus on converters within the EV domain, we have tailored our introduction to provide a comprehensive overview of our innovative solution, minimizing redundant information commonly known about EVs. The developed hybrid converter, designed with a primary dedication to EV applications, transcends conventional boundaries by offering a versatile solution for a range of scenarios.

Beyond EVs, its applications extend to DC micro-grids and the seamless integration of renewable energy resources into electric grids. This adaptability is achieved through a sophisticated architecture, featuring a diode bridge rectifier, coupled SEPIC, and flyback converters. The integration of two auxiliary switches further elevates the converter's flexibility, allowing dynamic selection between SEPIC, flyback, or a hybrid mode to suit diverse operational requirements. This paper explores specific duty cycles for each switch, leveraging mathematical calculations grounded in circuit parameters. This in-depth analysis ensures optimal performance across varied operational modes, emphasizing the practical utility and adaptability of our converter to meet the unique demands of EV applications [23]-[25].

One study examines the direct power control (DPC) technique for three-phase PWM AC-DC converters under unbalanced voltage conditions. It highlights how such conditions can lead to significant performance degradation due to the presence of negative voltage components in the grid, which adversely affect the operation of grid-connected VSIs. By modifying the conventional DPC input structures with simpler sequence networks, the study achieved a 70% improvement in input power under unbalanced conditions, measured through a reduction in THD [26]. Another research paper extends this work by emphasizing the necessity of addressing symmetrical components to mitigate the adverse effects of unbalanced voltage, improving power quality and reducing THD [27].

A different approach involves the analysis of virtual flux direct power control (VFDPC) for AC-DC converters. This technique eliminates the need for voltage sensors by estimating grid virtual flux based on converter switching states, line current, and DC-link output voltage. This method not only simplifies the control system but also achieves low harmonic distortion (below 5%) and near unity power factor, making it highly suitable for EV applications [28]. Additionally, another study proposes a two-stage bidirectional AC-DC converter utilizing wavelet modulation for EV charging systems. The results demonstrate a significant reduction in output voltage ripple and harmonic distortion, enhancing the overall performance of the charging infrastructure [28].

The paramount objective of the proposed hybrid converter is to address the following issues:

- Integrated SEPIC and flyback converters: the combination allows the converter to switch between SEPIC and flyback modes or use both simultaneously. This flexibility optimizes performance under varying load conditions, which is not typically seen in conventional topologies.
- Auxiliary controlled switches: these additional switches provide a mechanism to dynamically select the optimal mode of operation. This is a unique feature that differentiates your design from more static approaches in traditional and integrated converters.
- Reduced THD: the proposed converter achieves a THD of 14.51%, which is lower than many existing hybrid converters. This improvement in THD directly contributes to better power quality and more efficient operation.
- Efficiency improvements: at rated load conditions, the proposed converter reaches 90% efficiency. Discuss how the integration of SEPIC and flyback converters, along with the auxiliary switches, contributes to this high efficiency.
- Flexibility in application: by accommodating different operational modes (SEPIC, flyback, or a combination), the converter can be tailored to specific applications like DC micro-grids or EV installations, providing superior adaptability compared to single-mode converters.
- Improved power factor: highlight how the reduction in THD contributes to an improved power factor, making the proposed converter more suitable for sensitive applications where power quality is critical.

The rest of the paper is organized as follow. Section 1 introduces the paper. Section 2 discusses the proposed hybrid converter. Section 3 discusses the simulation results. Section 4 discusses the ability of the proposed converter to improve the grid current power factor. Finally, section 5 concludes the paper.

## 2. THE PROPOSED HYBRID CONVERTER

Figure 1 shows the improved hybrid AC-DC converter. It comprises of conventional diode bridge rectifier, two DC-DC converters (flyback and SEPIC converters), one main switch  $M_1$ , two additional switches  $A_1$  and  $A_2$  and low pass filter capacitor  $C_o$  (This capacitor represents  $C_f$  or  $C_s$ ). The use of two DC-DC converters, without introducing two auxiliary switches, is proposed in [22]. In this paper, the improved hybrid AC-DC converter is dedicated to EVs applications. To charge the main and auxiliary storage system in EVs

from electrical grids, such configuration must be used. However, due to non-linearity of output capacitance behavior of the semiconductor switches at high switching frequency in the circuit, the power factor of the line current will be smashed. Therefore, two auxiliary switches are inserted as seen in Figure 1 to reduce the THD in the line current (the input voltage of Figure 1 is rectified voltage by diode bridge rectifier. The condition of  $A_1$  and  $A_2$  determines the combination of the two converters (flyback or flyback/SEPIC). The operation mode is defined by the condition of  $A_1$  and  $A_2$ . As a result, the switching frequency of the auxiliary switches is substantially lower than the switching frequency of the main switch  $M_1$ . Therefore, additional two auxiliary switches are switched at grid frequency (50 Hz or 60 Hz) to reduce the switching losses, because these losses increase dramatically with the switching frequency [29], [30]. Second, these switches are used to select the operated DC-DC converter. Conducted a comprehensive review of three-port DC-DC converters' topologies for integrating renewable energy and energy storage systems. Their work delves into various converter configurations, shedding light on the evolving landscape of sustainable energy integration. The authors analyze the strengths and limitations of different topologies, contributing valuable insights to the ongoing efforts in advancing renewable energy technologies.

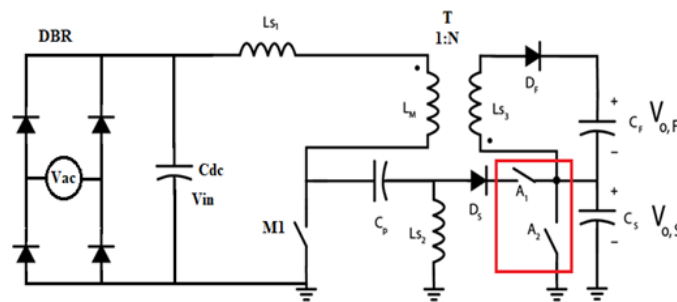


Figure 1. The proposed hybrid AC-DC converter

## 2.1. Modes of operations

The proposed hybrid converter has a number of moods of operation depending on the status of switches  $M_1$ ,  $A_1$ , and  $A_2$ . For simplicity, all devices are assumed to be ideal. The analysis is discussed in the following detail.

- Mode 1 ( $M_1$  is on  $A_1$  is off and  $A_2$  is off): Figure 2 shows the first two modes. During this mode, SEPIC and flyback inductors are energized through the current path shown in Figure 2(a).

When  $M_1$  is on, then,  $V_{ds} = 0$ , (ideal switch), applying KVL over the left loop of Figure 2(a):

$$V_{in} + V_{Ls1} + V_{LM} = 0, 0 < t < T_{on} \quad (1)$$

then,  $V_{Ls1} = V_{in} - V_{LM}$ . Therefore,  $i_{Ls1} = i_{LM}$  and has a linear ramp. Then, the current is given by:

$$i_{Ls1max} = \frac{V_{in}}{L_{s1} + L_M} DT_s \quad (2)$$

and the voltage of SEPIC inductor is equal to the voltage across the coupling capacitor. It means that:

$$V_{Ls2} = V_p \quad (3)$$

The current of  $L_{s2}$  is given by:

$$i_{Ls2max} = -\frac{V_{cp}}{L_{s2}} DT_s \quad (4)$$

- Mode 2 ( $M_1$  is off  $A_1$  is off and  $A_2$  is off): this mode represents the resonance mode between the parasitic capacitance of the main switch and the other passive components in the circuit. See Figure 2(b). This mode is too short compared to switching time, so it can be ignored.

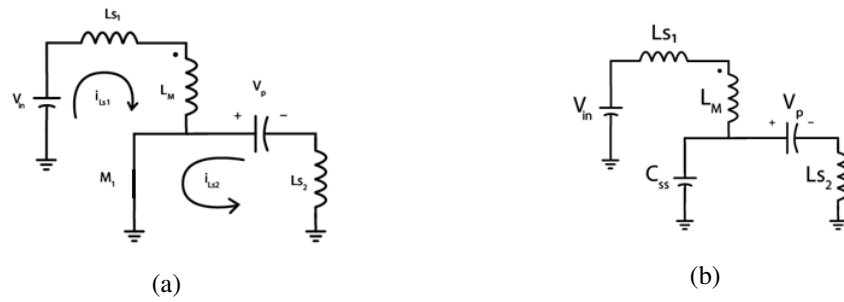


Figure 2. The equivalent circuit the first two modes (a) mode 1 and (b) mode 2

- Mode 3 ( $M_1$  is off  $A_1$  is off and  $A_2$  is on): based on Figure 3, during this mode, the energy is transferred through the flyback diode to output capacitor. Whereas the SEPIC output capacitance is discharged through the auxiliary switch  $A_2$ , see Figure 3(a).

The load voltage is given by (keep in mind the transformer turns ratio is  $a$ ):

$$V_o = \frac{V_{in}}{a} = V_{Ls3} \quad (5)$$

Writing the current in secondary side of the transformer, this is given by:

$$i_{Ls3} = \frac{V_{Ls3}}{L_{s3}}(1 - D)K_2T_s \quad (6)$$

Where  $K_2=1-K_1$ , is the duty cycle of  $A_2$ ,  $V_{Cf} = V_{o,f}$  and  $i_{Ls3} = ai_{Ls1}$ .

- Mode 4 ( $M_1$  is off  $A_1$  is on and  $A_2$  is off): during this mode, the converter operates as boost converter. See Figure 3(b). The currents during this mode are given by, respectively:

$$i_{Ls1min} = \frac{(V_{in} - V_{Cp} - V_{o,s})}{(L_{s1} + L_M)}(1 - D)T_sK_1 \quad (7)$$

$$i_{Ls2min} = \frac{V_{o,s}}{L_{s2}}(1 - D)T_sK_1 \quad (8)$$

Where  $K_1$  is the duty cycle of switch  $A_1$ ,  $V_{Ls2}=V_{o,s}$ , and  $i_{Ls1}$ = Same as mode 3.

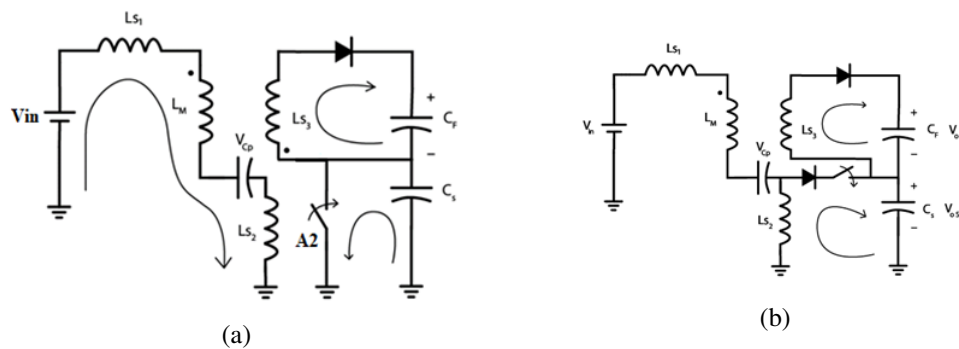


Figure 3. The equivalent circuit the first two modes (a) mode 3 and (b) mode 4

## 2.2. Duty cycles derivation

To drive the main switch duty cycle  $M_1$ , starting from the condition  $i_{Ls1-mode1}=i_{Ls1-mode3}$ , this gives:

$$\frac{V_{in}}{L_{s1} + L_M}DT_s = \frac{V_{in}}{a^2L_{s3}}(1 - D)T_s \quad (9)$$

Solve for  $D$ , this yields:

$$D = \frac{1}{a^2 L_{s3}} \frac{1}{\left[ \frac{1}{L_{s1} + L_M} + \frac{1}{a^2 L_{s3}} \right]} \quad (10)$$

to drive the switch  $A_1$  duty cycle, this condition must be satisfied.

$$i_{L_{s1-mode3}} = i_{L_{s1-mode4}} \quad (11)$$

Then,

$$\frac{V_{in}}{a^2 L_{s2}} (1 - D) T_s = \frac{V_{in} - V_{Cp} - V_{o,s}}{L_{s2} + L_M} (1 - D) T_s K_1 \quad (12)$$

$$\frac{V_{in}}{a^2 L_{s2}} (1 - K_1) = \frac{V_{in} - V_{Cp} - V_{o,s}}{L_{s2} + L_M} K_1 \quad (13)$$

solve for  $K_1$  gives:

$$K_1 = \left[ \frac{V_{in}}{a^2 L_{s2}} \right] \frac{1}{\left[ \frac{V_{in} - V_{Cp} - V_{o,s}}{L_{s2} + L_M} + \frac{V_{in}}{a^2 L_{s2}} \right]} \quad (14)$$

it should be noted that  $A_1$  and  $A_2$  are both complementary to each other.

The effective duty cycle in power electronics converters can notably increase during high-frequency operations due to turn-off and turn-on delay mismatches. This phenomenon arises from a misalignment between the idealized switching events and the actual timing in practical applications. The consequence is an elevated effective duty cycle, which significantly affects the converter's performance, especially at higher switching frequencies. Turn-off and turn-on delay mismatches become particularly pronounced with increased switching frequencies, posing challenges in accurately controlling the duty cycle. This discrepancy can result in variations in the expected output and efficiency of the converter, underscoring the necessity for a thorough understanding and mitigation of these effects.

The consideration of turn-off and turn-on delay mismatches has been extensively explored in the literature, particularly in studies focusing on datasheet-driven modeling of power electronics converters. Mahafzah *et al.* [31], authors present a noteworthy contribution in the realm of power electronics with their duty cycle regulation based PWM control for a five level flying-capacitor inverter. This work addresses the intricacies of control mechanisms in multilevel inverters, showcasing advancements in power electronics research and application.

### 2.3. Parameters design and selection

The continuous conduction mode is selected to operate the proposed converter. It supplies a 4.5 kW load at 20 kHz switching frequency of switch  $M_1$  and 50 Hz grid frequency of both auxiliary switches  $A_1$  and  $A_2$ . The selected the proposed converter components are computed as the following steps:

- The magnetization inductance ( $L_m$ ) is designed to reduce the ripple in the primary current. Therefore, reducing the design complexity of the circuit's EMI filter [25]. The lower limit for this inductance is:

$$L_{m-min} = \frac{(1 - D)^2 R_o}{2f_s} \quad (15)$$

where  $f_s$  is the switching frequency, and  $R_o$  is the load resistance.

- The flyback output capacitance  $C_o$  plays an important role in reducing the output voltage ripple, set the poles of the system transfer function, and imply the response of the supply to a sudden large change of the load current [29]. The minimum limit of flyback output capacitance is calculated by:

$$C_{o,f-min} = \frac{D}{\frac{\Delta V_o}{V_o} R_o f_s} \quad (16)$$

where,  $\frac{\Delta V_o}{V_o}$  is the required output voltage ripple of the flyback.

- The transformer turns ratio ( $a = \frac{N_1}{N_2}$ ) is set to determine the proposed converter duty cycle of the flyback converter [29]. This reduces the flyback diode voltage stress and the voltage stress on output capacitance. Then, the turns ratio can be calculated by:

$$a = \frac{N_1}{N_2} = \frac{V_{in} D_{max}}{V_{o,f}(1 - D_{max})} \quad (17)$$

- The SEPIC inductance  $L_{s2}$  are designed to make the EMI filter is simpler [30]. The inductance is given by:

$$L_{s2} = \frac{V_o(1 - D)}{\Delta I_{s2} f_s} \quad (18)$$

where  $\Delta I_{s2}$  is the desired current ripple in  $L_{s2}$ .

- The SEPIC output capacitance  $C_{o,s}$  is designed to be:

$$C_{o,s-min} = \frac{\Delta I_2}{8 \Delta V_{o,s} f_s} \quad (19)$$

- The SEPIC capacitance  $C_p$  is designed to pass through a high RMS current when it is compared to  $C_{o,s}$ , therefore, it should be selected to be (where  $L_{eq}$  is the equivalent of parallel inductance  $L_M$  and  $L_{s3}$ ):

$$C_{p-min} = \frac{L_{eq} I_2^2}{2 \Delta V_{c-p}} \quad (20)$$

- The suggested converter is designed for medium power applications with a rated power of 4.5 kW to demonstrate its functionality. Thus, system characteristics such as input/output power, input/output voltages, and switching frequency are specified; the other parameters are determined using the mathematical model provided thus far.
- Switching frequency derivation: However, to drive the switching frequency of the proposed converter the following steps should be followed: based on (2) and (4), if  $M_1$  is on, the drain current is given by:

$$I_M = L_{s1} + L_{s2} \quad (21)$$

$$I_M = \frac{V_{in}}{(L_{s1} + L_M)} T_{on} - \frac{V_{cp}}{L_{s2}} T_{on} \quad (22)$$

solving for  $T_{on}$  gives:

$$T_{on} = \frac{I_M}{\frac{V_{in}}{(L_{s1} + L_M)} - \frac{V_{cp}}{L_{s2}}} \quad (23)$$

and based on (7), solving for  $T_{off}$  gives:

$$T_{off} = \frac{I_{Ls1}}{K_1 \frac{V_{in} - V_{cp} - V_{o,s}}{L_{s1} + L_M}} \quad (24)$$

therefore, the converter switching time is  $T_s = T_{on} + T_{off}$ :

$$T_s = \frac{I_M}{\frac{V_{in}}{(L_{s1} + L_M)} - \frac{V_{cp}}{L_{s2}}} + \frac{I_{Ls1}}{K_1 \frac{V_{in} - V_{cp} - V_{o,s}}{L_{s1} + L_M}} \quad (25)$$

## 2.4. Voltage control loops

The proposed converter needs two separate control loops (Figure 4). The first one to control the main switch,  $M_1$  as seen in Figure 1. To keep the output voltage within the acceptable limit ( $V_{ref}$ ), a very simple voltage control loop is used. The observed feedback voltage is compared to a reference voltage, as shown in Figure 4(a). The PI controller is used to lower the comparison stage's steady state inaccuracy. The duty cycle of the main switch is the output of the PI controller stage. The gate to source voltage of the chosen MOSFET is then generated using the PWM generator at a given switching frequency ( $f_s$ ). In summary, see Figures 4(a), 4(b), and results of control loop are seen in Figure 5.

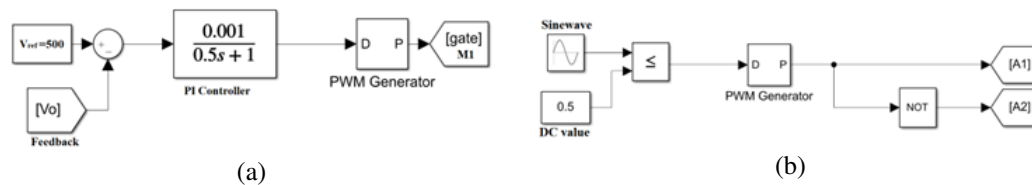


Figure 4. The output voltage control (a) the first control loop and (b) the second control loop

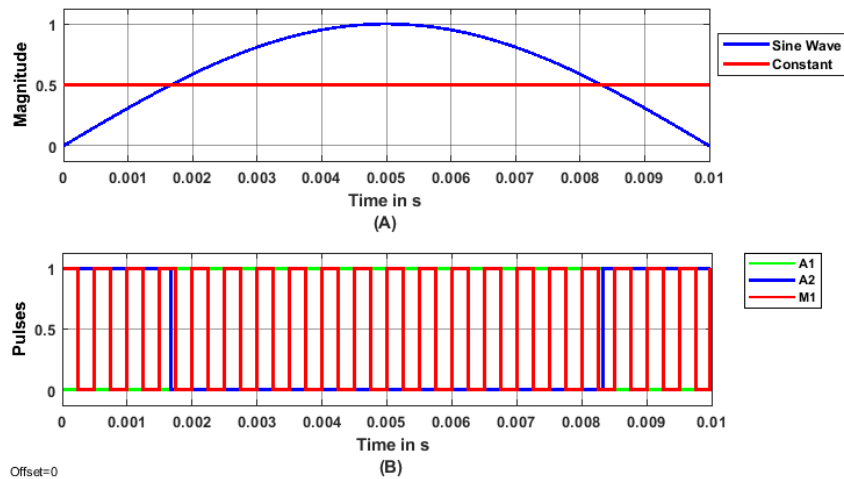


Figure 5. Results of control loops (a) auxiliary switches selection condition and (b) pulses of all switches

Finally, the auxiliary switches do not affect the converter losses because they are operating at 50 Hz (grid frequency), therefore, the associated losses are negligible. The determination of controller gains within the PI controller plays a key role in achieving stable and responsive control of the hybrid AC-DC converter. Within the voltage control loop governing the main switch ( $M_1$ ), the PI controller serves to minimize steady state inaccuracies by comparing the observed feedback voltage to the reference voltage ( $V_{ref}$ ). The proportional (P) component of the PI controller addresses immediate errors, while the integral (I) component focuses on persistent offsets, collectively enhancing the controller's proficiency in maintaining the desired output voltage. Selecting appropriate gains for the PI controller involves a precise tuning process, balancing the need for rapid responses to sudden system changes and the elimination of long term voltage discrepancies. This tuning is typically achieved through iterative processes, simulation studies, or empirical testing, ensuring optimal controller performance. The strategic selection of PI controller gains is equally crucial for the secondary control loop overseeing the auxiliary switches ( $A_1$  and  $A_2$ ). Here, the PI controller contributes to maintaining equilibrium between the sinusoidal waveform and the DC value, facilitating effective gating of the auxiliary switches. Analogous to the voltage control loop, the proportional and integral gains of the PI controller in this context require precise tuning for swift responses to changes in the sinusoidal waveform and accurate control over the operation of the auxiliary switches. This detailed tuning process is instrumental in achieving the desired performance characteristics of the proposed hybrid AC-DC converter, ensuring a dynamic response to system changes and precise regulation of both main and auxiliary switches.



Mahafzah *et al.* [32], authors conduct a thorough review and comparison of integrated inductive-based hybrid step up DC-DC converters under continuous conduction mode (CCM). The paper contributes valuable insights into the design and performance evaluation of hybrid converters. The authors' work aids in the understanding of integrated inductive based converters, offering a basis for further advancements in DC-DC conversion technology. Moving on to [33], authors introduce a novel synchronized multiple output DC-DC converter based on hybrid flyback-Cuk topologies. Their work addresses the need for efficient and synchronized power conversion, providing a solution that combines the benefits of flyback and Cuk topologies. This novel approach holds promise for enhancing the performance and reliability of DC-DC converters in various applications. Yan *et al.* [34], authors focus on adaptive PI control for the speed regulation of a DC motor. Their work introduces a reinforcement learning algorithm for adaptive control, exhibiting potential in achieving precise and adaptable speed control for DC motors. Moving beyond controller considerations, an in-depth analysis of voltage and current stresses is important for a comprehensive evaluation of the proposed hybrid AC-DC converter. This process involves exploring stress factors inherent in the converter's unique architecture and diverse operational modes. Investigating voltage stresses, which include peak and RMS voltages, will provide crucial insights into their implications on overall performance and reliability. Simultaneously, current stresses involve an assessment of peak and RMS current levels, shedding light on potential challenges and optimizing the operational efficiency of the converter. Zeng *et al.* [35], authors present a DC capacitor-less inverter for single-phase power conversion with minimized voltage and current stress. Their work addresses the challenges associated with traditional DC capacitors in inverters. The proposed solution offers a promising alternative, minimizing stress on both voltage and current in single-phase power conversion applications. Mahafzah *et al.* [36], contribute to the field of inverter reliability estimation by automating component level stress measurements. Their work focuses on advancing the methodologies for assessing the reliability of inverters. The authors' automated stress measurement approach enhances the efficiency of reliability estimation, marking a significant step forward in the field of inverter technology.

### 3. SIMULATION RESULTS

This section presents the simulation results of the proposed converter, see Figure 6, validated using MATLAB/Simulink R2020a. The maximum step size is set to 25 ms, and the solver utilized is an ordinary differential equation (ODE23tb) with a relative tolerance of  $10^{-3}$ . With a simulation time of 1s, the proposed converter is expected to reach a steady state. The simulation results for the proposed converter are elaborated upon in this section. Parameters are chosen based on the preceding discussion, with minor adjustments as outlined in Table 1, summarizing the parameters selected for the 4.5 kW power application employed in the simulation. These characteristics are suitable for various applications, including EVs adapters, micro-inverter applications, and the integration of hybrid renewable energy resources with power systems.

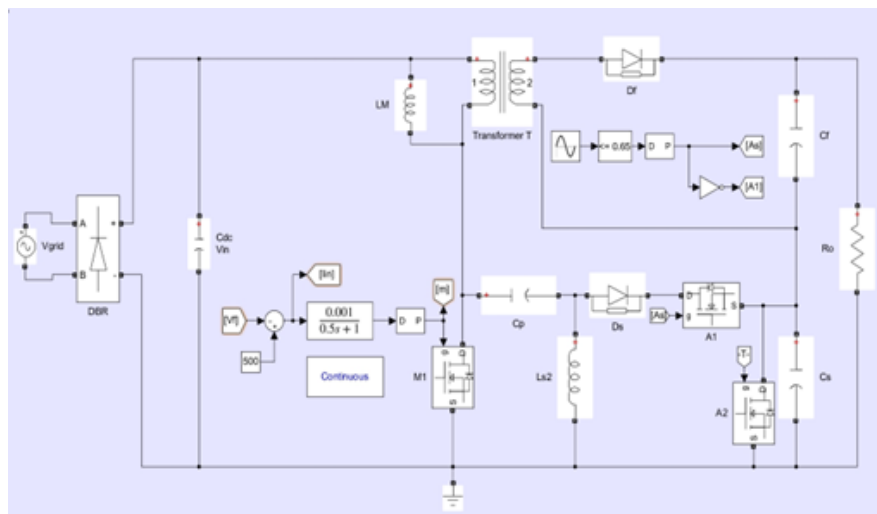


Figure 6. Overall simulated system

The simulated load voltage and current are shown in Figure 7. As shown, the load voltage (Figure 7(a)) is a DC voltage with value around 500 V with the ripple in the voltage is about 12%. The load current is adopted in Figure 7(b). It has the same behavior as the load voltage. The average load current is about 8.5 A, which is sufficient to charge the EV auxiliary system. Due to switching behavior of the used converter during charging the auxiliary batteries of EVs from the electrical grid, this increases the nonlinear loads are connected to the grid. Therefore, the line current suffers from high THD. The improved hybrid converter can operate as a power factor correction topology because of its ability to form the line current and reduce its THD (see Figure 8). As expected, the improved converter can form a nearly sinusoidal grid current wave, see Figure 8(a), with a THD within a standard (see IEEE-519). It can be seen from Figure 8(b) that the grid current has THD about 14.51%. The individual 3rd harmonic has the main contribution. It has a magnitude of 13.2%. However, if the used filter is optimally designed, this value will be further reduced.

Table 1. Simulation parameters

Variable	Description	Value
$P_{in}/P_o$	Input/Output power	4.5 kW
$V_{in}$	RMS grid voltage	220 V-rms
$V_o$	Output DC voltage	500 V
$I_o$	Output DC current	8.5 A
$a$	Transformer ratio	350/1,000
$C_p$	SEPIC coupling capacitor	720 $\mu$ F
$L_{s2}$	SEPIC second inductor	800 $\mu$ H
$C_s$	SEPIC filter capacitor	520 $\mu$ F
$C_f$	Flyback filter capacitor	720 $\mu$ F

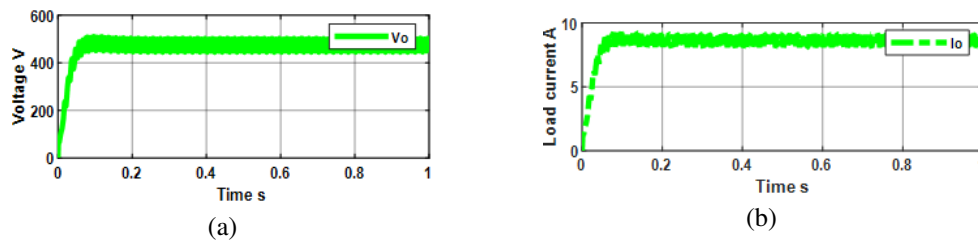


Figure 7. Simulated voltage and current; (a) the load voltage and (b) the load current

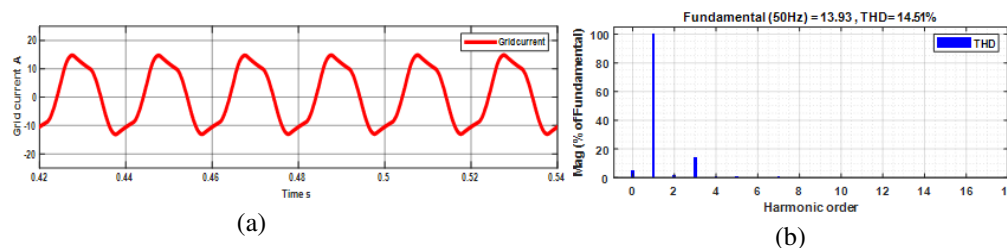


Figure 8. Simulated line current and THD; (a) the grid current and (b) THD of the grid current

#### 4. POWER FACTOR CORRECTION IN THE GRID CURRENT AND EFFICIENCY CALCULATION

The power factor of the grid current has become a main concern in recent years. However, Figure 8(b) depicts THD of a grid current. The THD of the line current in Figure 8(a) is around 14.51% when utilizing the fast fourier transform (FFT) tool in MATLAB. Due to inserting the auxiliary switches, the THD value has been reduced by about 3% compared with THD of the grid current of the hybrid SEPIC-Flyback converter proposed in [22].

The distortion factor of the line current is given by:

$$DF = \frac{1}{\sqrt{1 + THD^2}} \quad (26)$$

As the load of the converter is pure DC, its  $\cos\theta = 1$ . Where the power factor can be estimated by:

$$PowerFactor = DF * \cos\theta \quad (27)$$

By applying (26) and (27), the power factor of the grid current when utilizing the proposed hybrid converter in this paper is calculated to be 98.96%. Upon closer examination of the harmonic components of both currents, as illustrated in Figure 8(b), it becomes evident that THD can be further reduced by implementing a robust input filter to mitigate the third harmonic component. Consequently, by properly attenuating the relevant EMI filter, these values can be diminished. It is noteworthy that the power factor of the line current is low in both cases of line voltage and necessitates rectification. This issue is earmarked for future resolution.

Finally, The efficiency of the proposed converter can be calculated by calculating the different components of losses in the proposed circuit [29], [30]. To achieve the maximum efficiency of the proposed converter, both auxiliary switches  $A_1$  and  $A_2$  are operated at 50 Hz. The proposed converter efficiency as a function of duty cycle of  $M_1$  is plotted in Figure 9. It is clear that efficiency increases as a duty cycle is increased. At 0.2 duty cycle, the efficiency 65% and it reaches about 90% at 0.95 duty cycle of the main switch.

$$\eta = \frac{P_{out}}{P_{out} + P_{losses}} \quad (28)$$

Where  $P_{out}$  is the output power of the proposed converter and  $P_{losses}$  is the total losses in the proposed converter. Conventionally, the loss types in converters are conduction losses, switching losses, and control losses [29], [30]. To achieve the maximum efficiency of the proposed converter, both auxiliary switches  $A_1$  and  $A_2$  are operated at 50 Hz. The losses components are: conduction, switching and control losses.

#### 4.1. Conduction losses

During the conduction period of the main switch  $M_1$  and main diodes  $D_f$  and  $D_s$ , the conduction losses can be calculated as follows:

$$P_{conM1} = \frac{R_{on} V_{in}^2}{2DR_l^2} \quad (29)$$

where  $R_{on}$  is the MOSFET on-state resistance and  $R_l$  is the PCB series resistance of the current loop. Then,

$$P_{condDx} = \frac{V_x V_{in}^2}{4V_o R_1} \quad (30)$$

where  $D_x$  denotes the fly-back diode or SEPIC diode, and  $V_x$  denotes the forward voltage of fly-back or SEPIC diode.

#### 4.2. Switching losses

The switching losses in the main switch  $M_1$  is given by:

$$P_{swM1} = 0.5f_s C_{oss} (0.5V_{in} + V_o)^2 \quad (31)$$

where  $C_{oss}$  is the main switch output non-linear capacitance which depends on the applied drain source voltage. The combination of the two converters is selected based on the status of  $A_1$  and  $A_2$ . For this reason, the switching frequency of the auxiliary switches is much lower than that of the main switch  $M_1$ , i.e., 50 Hz. Therefore, they have no loss effect. The losses are computed based on the equations presented in [29], [33]. Then, the switching losses of the converters diodes are given by:

$$P_{swDx} = 0.5f_s C_d (0.5V_{in} + V_o)^2 \quad (32)$$

where  $D_x$  denotes the fly-back diode or SEPIC diode, and  $V_x$  denotes the forward voltage of fly-back or SEPIC diode.

### 4.3. Control losses

These losses are caused due to charging/discharging the input capacitance of the main switch. These losses can be calculated by:

$$P_{g-M1} = 2Q_{g-M1}V_{g-M1}f_s \quad (33)$$

where  $Q_{g-M1}$  is main switch gate charge and  $V_{g-M1}$  is the voltage needed to charge the  $M_1$  gate.

### 4.4. Transformer losses

The electrical losses in the fly-back transformer is divided in two main components: first core losses are ignored because the core is assumed to be ideal. Second the copper losses in the windings which considered in the conduction losses. Finally, the total losses in the proposed converter can be given by:

$$P_t = P_{conduction} + P_{switching} + P_{control} \quad (34)$$

The proposed converter efficiency as a function of duty cycle of  $M_1$  is plotted in Figure 9. It is clear that efficiency increases as a duty cycle is increased. At 0.2 duty cycle, the efficiency 65% and it reaches about 90% at 0.95 duty cycle of the main switch.

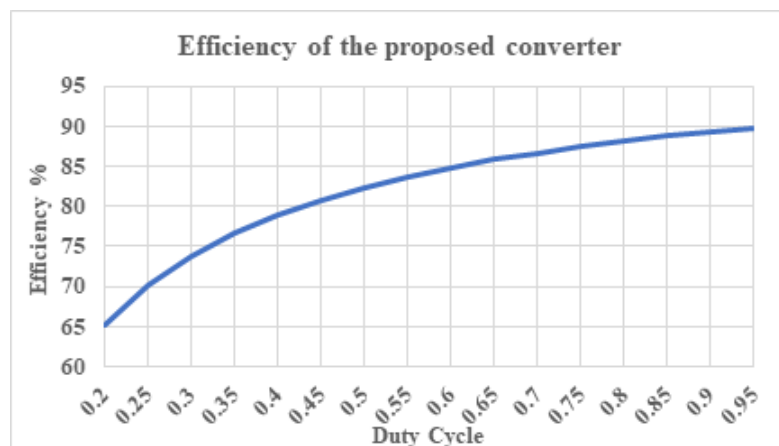


Figure 9. The proposed converter efficiency verses duty cycle of  $M_1$

## 5. CONCLUSION

This paper developed a novel hybrid AC-DC converter that is intended for use in a variety of applications such as DC micro-grids, EV installations, and the integration of renewable energy resources into electric grids. A diode bridge rectifier, two coupled SEPIC and flyback converters, and two additional auxiliary controlled switches are used in the proposed hybrid converter. These additional switches allow you to choose between SEPIC, flyback, or a mix of the two. The paper goes into the operational modes in detail, utilizing mathematical calculations to calculate specific duty cycles for each switch based on the circuit parameters. The aim of this hybrid converter is to reduce THD in the line current. The results demonstrate a THD of around 14.51%, a 3% reduction compared to previous hybrid converters, consequently improving the power factor of the line current. Moreover, the proposed converter reaches 90% efficiency at rated load conditions. To evaluate the functionality of the proposed hybrid converter, a 4.5 kW converter is simulated and conducted using MATLAB/Simulink once the relevant passive parameters are configured.

## FUNDING INFORMATION

Authors state there is no funding involved.

## AUTHOR CONTRIBUTIONS STATEMENT

This journal uses the Contributor Roles Taxonomy (CRediT) to recognize individual author contributions, reduce authorship disputes, and facilitate collaboration.

Name of Author	C	M	So	Va	Fo	I	R	D	O	E	Vi	Su	P	Fu
Khaled A. Mahafzah	✓	✓	✓	✓						✓				
Mohamad A. Obeidat	✓	✓	✓	✓						✓				
Hesham Alsalem	✓	✓	✓	✓						✓				
Ayman Mansour	✓	✓	✓	✓						✓				
Eleonora Riva Sanseverino	✓	✓	✓	✓						✓				

C : Conceptualization

M : Methodology

So : Software

Va : Validation

Fo : Formal Analysis

I : Investigation

R : Resources

D : Data Curation

O : Writing - Original Draft

E : Writing - Review & Editing

Vi : Visualization

Su : Supervision

P : Project Administration

Fu : Funding Acquisition

## CONFLICT OF INTEREST STATEMENT

Authors state no conflict of interest.

## DATA AVAILABILITY

Data availability is not applicable to this paper as no new data were created or analyzed in this study.




## REFERENCES

- [1] Z. Li, A. Khajepour, and J. Song, "A comprehensive review of the key technologies for pure electric vehicles," *Energy*, vol. 182, pp. 824–839, Sep. 2019, doi: 10.1016/j.energy.2019.06.077.
- [2] R. Chen, J. Zeng, X. Huang, and J. Liu, "An H filter based active damping control strategy for grid-connected inverters with LCL filter applied to wind power system," *International Journal of Electrical Power & Energy Systems*, vol. 144, p. 108590, Jan. 2023, doi: 10.1016/j.ijepes.2022.108590.
- [3] X. Sun, Z. Li, X. Wang, and C. Li, "Technology development of electric vehicles: a review," *Energies*, vol. 13, no. 1, p. 90, Dec. 2019, doi: 10.3390/en13010090.
- [4] H. Kun, C. Rong, Z. Jingtao, G. Xundong, and H. Guodong, "Analysis of current protection in distribution networks with clean energy access," *Frontiers in Energy Research*, vol. 10, Jan. 2023, doi: 10.3389/fenrg.2022.1035781.
- [5] M. A. Obeidat, O. Alsmeerat, A. M. Mansour, and J. Abdallah, "Reducing the fluctuations effect of the DC supply on the three phase inverter using intelligent inverter control," *WSEAS TRANSACTIONS ON POWER SYSTEMS*, vol. 17, pp. 224–233, Jul. 2022, doi: 10.37394/232016.2022.17.23.
- [6] C. Zhang, J. Jasni, M. A. M. Radzi, N. Azis, and X. He, "A comprehensive review of stage-of-the-art subsystems configurations, technical methodologies, advancements, and prospects for new energy electric vehicles," *Ionics*, vol. 29, no. 7, pp. 2529–2547, Jul. 2023, doi: 10.1007/s11581-023-05062-3.
- [7] A. K. Venkitaraman and V. S. R. Kosuru, "Trends and challenges in electric vehicle motor drivelines - a review," *International Journal of Electrical and Computer Engineering Systems*, vol. 14, no. 4, pp. 485–495, 2023, doi: 10.32985/ijeces.14.4.12.
- [8] S. Abdul Yamin, "A review of electric vehicle challenges in Malaysia," *9th International Conference LIS (Liga Ilmu Serantau) 2023: Digital Transformation Towards Infinite Possibility*, pp. 2985–4393, 2023.
- [9] C. Dhanamjayulu, S. Padmanaban, V. K. Ramachandaramurthy, J. B. Holm-Nielsen, and F. Blaabjerg, "Design and implementation of multilevel inverters for electric vehicles," *IEEE Access*, vol. 9, pp. 317–338, 2021, doi: 10.1109/ACCESS.2020.3046493.
- [10] G. Chacko, L. Syamala, N. James, B. M. Jos, and M. Kallarackal, "Switching frequency limited hysteresis based voltage electric vehicles: the role and importance of standards in an emerging market," *Energies*, 2023.
- [11] A. Shawky, M. A. Sayed, and T. Takeshita, "Analysis and experimentation of modular differential inverter utilizing SEPIC modules and SIC devices for grid connected applications," *IEEE Journal of Industry Applications*, vol. 9, no. 5, pp. 573–583, Sep. 2020, doi: 10.1541/iejia.9.573.
- [12] N. Takaoka, H. Watanabe, and J. Itoh, "Isolated DC to single-phase AC converter with active power decoupling capability using coupled inductor," *Journal of the Institute of Electrical Engineers of Japan*, vol. 142, no. 10, pp. 1123–1131, Mar. 2021, doi: 10.1541/iejia.21004506.
- [13] C. Larouci, T. Azib, A. Chaibet, and M. Boukhniifer, "Control of a flyback converter in mixed conduction mode: influence on the converter design using optimization under constraints," *Journal of Power Electronics*, vol. 12, no. 4, pp. 623–632, 2012.
- [14] R. Parekh, "AC induction motor fundamentals," *Microchip Technology Inc*, pp. 1–24, 2003, [Online]. Available: <http://jimfranklin.co.uk/microchipdatasheets/00887a.pdf>.
- [15] K. Thiagarajan and T. Deepa, "A comprehensive review of high-frequency transmission inverters for magnetic resonance inductive wireless charging applications in electric vehicles," *IETE Journal of Research*, vol. 69, no. 5, pp. 2761–2771, Jul. 2023, doi: 10.1080/03772063.2021.1905089.

- [16] D. Zhao, C. Guo, Y. Li, S. Pan, S. Feng, and H. Zhu, "Study of the temperature distribution in insulated gate bipolar transistor module under different test conditions," *Microelectronics Reliability*, vol. 140, p. 114880, Jan. 2023, doi: 10.1016/j.microrel.2022.114880.
- [17] K. Saadaoui, K. S. Rhazi, Y. Mejdoub, and A. Aboudou, "Modelling and simulation for energy management of a hybrid microgrid with droop controller," *International Journal of Electrical and Computer Engineering (IJECE)*, vol. 13, no. 3, p. 2440, Jun. 2023, doi: 10.11591/ijece.v13i3.pp2440-2448.
- [18] S. S. G. Acharige, M. E. Haque, M. T. Arif, N. Hosseinzadeh, K. N. Hasan, and A. M. T. Oo, "Review of electric vehicle charging technologies, standards, architectures, and converter configurations," *IEEE Access*, vol. 11, pp. 41218–41255, 2023, doi: 10.1109/ACCESS.2023.3267164.
- [19] K. A. Mahafzah and H. A. Rababah, "A novel step-up/step-down DC-DC converter based on flyback and SEPIC topologies with improved voltage gain," *International Journal of Power Electronics and Drive Systems (IJPEDS)*, vol. 14, no. 2, pp. 898–908, 2023, doi: 10.11591/ijpeds.v14.i2.pp898-908.
- [20] A. H. Okilly *et al.*, "Estimation technique for IGBT module junction temperature in a high-power density inverter," *Machines*, vol. 11, no. 11, p. 990, Oct. 2023, doi: 10.3390/machines11110990.
- [21] B. Tekgun, D. Tekgun, and I. Alan, "A multi-functional quasi-single stage bi-directional charger topology for electric vehicles," *Ain Shams Engineering Journal*, vol. 15, no. 3, p. 102471, Mar. 2024, doi: 10.1016/j.asej.2023.102471.
- [22] A. M. Lulhe and T. N. Date, "A technology review paper for drives used in electrical vehicle (EV) & hybrid electrical vehicles (HEV)," in *2015 International Conference on Control, Instrumentation, Communication and Computational Technologies (ICCICCT)*, Dec. 2015, pp. 632–636, doi: 10.1109/ICCICCT.2015.7475355.
- [23] J. A. Sanguesa, V. Torres-Sanz, P. Garrido, F. J. Martinez, and J. M. Marquez-Barja, "A review on electric vehicles: technologies and challenges," *Smart Cities*, vol. 4, no. 1, pp. 372–404, Mar. 2021, doi: 10.3390/smartcities4010022.
- [24] J. Van Mierlo *et al.*, "Beyond the state of the art of electric vehicles: a fact-based paper of the current and prospective electric vehicle technologies," *World Electric Vehicle Journal*, vol. 12, no. 1, p. 20, Feb. 2021, doi: 10.3390/wevj12010020.
- [25] A. Bouafia, J. P. Gaubert, and A. Chaoui, "Direct power control scheme based on disturbance rejection principle for three-phase pwm ac/dc converter under different input voltage conditions," *Journal of Electrical Systems*, vol. 8, no. 4, pp. 367–383, 2012.
- [26] U. Alejandro-Sanjines, A. Maisincho-Jivaja, V. Asanza, L. L. Lorente-Leyva, and D. H. Peluffo-Ordóñez, "Adaptive PI controller based on a reinforcement learning algorithm for speed control of a DC motor," *Biomimetics*, vol. 8, no. 5, p. 434, Sep. 2023, doi: 10.3390/biomimetics8050434.
- [27] R. Chen, Y. Liu, and F. Z. Peng, "DC capacitor-less inverter for single-phase power conversion with minimum voltage and current stress," *IEEE Transactions on Power Electronics*, vol. 30, no. 10, pp. 5499–5507, Oct. 2015, doi: 10.1109/TPEL.2014.2375271.
- [28] J. Flicker, J. Johnson, P. Hacke, and R. Thiagarajan, "Automating component-level stress measurements for inverter reliability estimation," *Energies*, vol. 15, no. 13, p. 4828, Jul. 2022, doi: 10.3390/en15134828.
- [29] K. Ma, W. Chen, M. Liserre, and F. Blaabjerg, "Power controllability of a three-phase converter with an unbalanced AC source," *IEEE Transactions on Power Electronics*, vol. 30, no. 3, pp. 1591–1604, Mar. 2015, doi: 10.1109/TPEL.2014.2314416.
- [30] A. M. Razali, M. A. Rahman, G. George, and N. A. Rahim, "Analysis and design of new switching lookup table for virtual flux direct power control of grid-connected three-phase PWM AC-DC converter," *IEEE Transactions on Industry Applications*, vol. 51, no. 2, pp. 1189–1200, 2015, doi: 10.1109/TIA.2014.2344503.
- [31] K. A. Mahafzah, K. Krischan, and A. Muetze, "Efficiency enhancement of a three phase Soft Switching Inverter under light load conditions," in *IECON 2016 - 42nd Annual Conference of the IEEE Industrial Electronics Society*, Oct. 2016, pp. 3378–3383, doi: 10.1109/IECON.2016.7793310.
- [32] K. A. Mahafzah, K. Krischan, and A. Muetze, "Efficiency enhancement of a three phase Hard Switching Inverter under light load conditions," in *IECON 2016 - 42nd Annual Conference of the IEEE Industrial Electronics Society*, Oct. 2016, pp. 3372–3377, doi: 10.1109/IECON.2016.7793732.
- [33] N. Zhang, D. Sutanto, and K. M. Muttaqi, "A review of topologies of three-port DC-DC converters for the integration of renewable energy and energy storage system," *Renewable and Sustainable Energy Reviews*, vol. 56, pp. 388–401, Apr. 2016, doi: 10.1016/j.rser.2015.11.079.
- [34] G. Yan, W. Liu, Y. Chen, Y. Wang, and J. Li, "Duty-cycle-regulation based PWM control of five-level flying-capacitor inverter 8.12," *Conference Proceedings - IPEMC 2004: 4th International Power Electronics and Motion Control Conference*, vol. 2, pp. 788–792, 2004.
- [35] W.-L. Zeng, C.-W. U, and C.-S. Lam, "Review and comparison of integrated inductive-based hybrid step-up DC-DC converter under CCM," in *2019 IEEE 62nd International Midwest Symposium on Circuits and Systems (MWSCAS)*, Aug. 2019, vol. 2019-Augus, pp. 730–733, doi: 10.1109/MWSCAS.2019.8885261.
- [36] K. A. Mahafzah, M. A. Obeidat, A. Q. Al-Shetwi, and T. S. Ustun, "A novel synchronized multiple output DC-DC converter based on hybrid flyback-cuk topologies," *Batteries*, vol. 8, no. 8, p. 93, Aug. 2022, doi: 10.3390/batteries8080093.




## BIOGRAPHIES OF AUTHORS






**Khaled A. Mahafzah, Dr. techn.,**    received a B.Sc. degree and M.Sc. degree in Electrical Power Engineering from the Department of Electrical Power Engineering at Yarmouk University, Irbid, Jordan, in 2010 and 2012, respectively. From 2012 to 2014 he served as a research and teaching assistant at the energy engineering department at German Jordanian University. In 2014 he started his Dr. techn., (Ph.D.) in power electronics and drives at the electrical drives and machines at Graz University of Technology, Austria. Currently, he is associate professor of power electronics and drives in electrical engineering department at Al-Ahliyya Amman University. His research interests are in power electronics, electrical drives, and the integrity of renewable engineering sources with power systems. He can be contacted at email: k.mahafzah@ammanu.edu.jo.








**Mohamad A. Obeidat**    (Member, IEEE), received the B.Sc. degree in electrical engineering from the Jordan University of Science and Technology, Jordan, in 1999, the M.Sc. degree in electrical engineering from Yarmouk University, Jordan, in 2006, and the Ph.D. degree in electrical engineering from Wayne State University, in 2013. He is currently a Professor in the Department of Electrical Power and Mechatronics Eng. and Vice-Dean of Scientific Research and Faculty of Graduate Studies, Tafila Technical University. He demonstrated excellent research and academic abilities and professional potentials. He has published several articles in the field of electrical engineering. His research interests include the field of intelligent control systems, renewable energy, intelligent systems, and mechatronics. He can be contacted at email: maobaidat76@ttu.edu.jo.






**Hesham Alsalem**    he obtained Ph.D. degree in Mechanical Engineering from Wayne State University, Detroit, MI, (USA) in 2016. He obtained a Master Degree in Mechanical Engineering from Jordan University of Science and Technology (Jordan) in 1999. And his Bachelor Degree in Mechanical Engineering from Jordan University of Science and Technology (Jordan) in 1996. His research interests are in the fields of automotive engineering, energy harvesting systems, electrical and hybrid vehicles, electrical motors, inverters and batteries. And lithium sulfur batteries. He teaches several bachelor-level courses for mechanical engineering/hybrid vehicle technology students. He can be contacted at email: hmanasreh\_10@ttu.edu.jo.



**Ayman Mansour**    his higher received his B.Sc. degree in Electrical Engineering from the University of Sharjah, UAE, in 2004, followed by an M.Sc. degree in Electrical Engineering from the University of Jordan, Jordan, in 2006, and a Ph.D. degree in Electrical Engineering from Wayne State University in 2012. He currently holds the position of Professor in the Department of Computer and Communication Engineering and serves as the Dean of Scientific Research and Faculty of Graduate Studies at Tafila Technical University. Prof. mansour has demonstrated exceptional research and academic abilities, as well as professional potential. He has published numerous articles in the field of intelligent systems. His research interests encompass intelligent control systems, renewable energy, intelligent systems, and mechatronics. He can be contacted at email: mansour@ttu.edu.jo.



**Eleonora Riva Sanseverino**    his higher received the Doctor and Ph.D. degrees in electrical engineering from the University of Palermo, Palermo, Italy, in 1995 and 2000, respectively. Since 1995, she has been working in the Research Group of Electrical Power Systems. After receiving the Ph.D. degree, she had a researcher position at the Department of Electrical Engineering in Palermo. She is currently an assistant professor of power systems at the University of Palermo. Her main research interest include the field of optimization methods for electrical distribution systems design, operation, and planning. She can be contacted at email: eleonora.rivasanseverino@unipa.it.